Confinement-Induced Symmetry Breaking of Interfacial Surfactant Layers

F. A. M. Leermakers,*,† L. K. Koopal,† T. P. Goloub,‡ A. W. P. Vermeer,§ and J. Kijlstra⊥

Laboratory of Physical Chemistry and Colloid Science, Wageningen University, Dreijenplein 6, 6703 HB Wageningen, The Netherlands, Department of Colloid Chemistry, St. Petersburg State University, St. Petersburg, 198904, Russia, Bayer CropScience AG, D-40789 Monheim, Germany, and Bayer Technology Services GmbH, D-51368 Leverkusen, Germany

Received: March 1, 2006

Interaction forces between mesoscopic objects are fundamental to soft-condensed matter and are among the prime targets of investigation in colloidal systems. Surfactant molecules are often used to tailor these interactions. The forces are experimentally accessible and for a first theoretical analysis one can make use of a parallel-plate geometry. We present molecularly realistic self-consistent field calculations for an aqueous nonionic surfactant solution near the critical micellization concentration, in contact with two hydrophobic surfaces. The surfactants adsorb cooperatively, and form a monolayer onto each surface. At weak overlap the force increases with increasing compression of the monolayers until suddenly a symmetry braking takes place. One of the monolayers is removed jump-like and as the remaining monolayer can relax, some attraction is observed, which gives way to repulsion at further confinement. The restoring of symmetry at strong confinement occurs as a second-order transition and the force jumps once again from repulsion to attraction. It is anticipated that the metastable branch of the interaction curve will be probed in a typical force experiment. Under normal conditions pronounced hysteresis in the surface force is predicted, without the need to change the adsorbed amount jump-like.

Introduction

Mesoscopic length scales can only persist in molecularly complex media due to a subtle balance of forces. While repulsive interactions keep the entities apart from each other, the attractive ones tend to draw them together. This interplay of attraction and repulsion is essential. For a rational design of, e.g., nanotechnological applications, it is important to know how one can manipulate these forces by molecular parameters.

Much is known about the fundamental forces that play a role in soft condensed matter.[1−3] In aqueous systems there are many factors that contribute to the overall force. For bare solid objects (colloids) there are typically repulsive electrostatic interactions working against the attractive van der Waals contribution.[4,5] The forces may be modified by molecules that adsorb onto the particles. For example, the addition of salt or ionic surfactants will change the electrostatic repulsion. When homopolymers are present one may expect to find steric repulsion (e.g., for interacting polymer brushes), bridging attraction (in the case of adsorption), or depletion attraction (in the absence of adsorption).[6] Soft objects such as membranes can interact through repulsive undulation forces.[7] On top of this there may be additional contributions, such as structural forces (hydration forces), which may have a nonmonotonic dependence of the separation between the surfaces.[1]

There are unifying concepts that help to rationalize the interactions and most importantly the sign of the interaction (i.e., repulsion versus attraction). The first notion is that intermolecular and surface forces should be related to entropic and/or energetic consequences of confinement. These contributions may conveniently be collected into a phenomenological, sometimes called Ginzburg−Landau−de Gennes,[8,9] free energy functional $\Omega(H)$ as an integral over some function f of an appropriate order parameter $\Psi(z)$ and its derivative $\nabla\Psi(z)$: $\Omega(H) = \int f((\Psi(z) - \Psi^b),\nabla\Psi(z))dz$, where z is a spatial coordinate and b refers to the order parameter in the bulk solution. Typically, one takes $z = 0$ halfway between the two surfaces which are positioned at $z = |H/2|$. The idea is that there exists a specific order parameter profile that corresponds to a minimal free energy Ω. This profile obeys the corresponding Euler−Lagrange equation. The optimized order parameter profile is used to compute $\Omega(H)$ and the free energy of interaction F^{int} follows from $F^{int}(H) = \Omega(H) - \Omega(\infty)$. When $F^{int}(H)$ is a decreasing function with the distance H between the surfaces, we have repulsive interactions and when it increases there is attraction. As long as the order parameter (and its derivatives) remains small (weak interaction), it is allowed to approximate the function f by a power series in its variables.[8,9] By taking the first terms of this series it is possible to actually formulate generic predictions that can be rationalized by using symmetry arguments.

We distinguish properties of the order parameter (i) from those of the surfaces (ii). The surface properties are introduced in the problem by the boundary conditions for Ω or equivalently for the Euler−Lagrange equation. (i) The order parameter can be either symmetric or antisymmetric with respect to the symmetry plane at $z = 0$. If $\Psi(-z) - \Psi^b = \Psi(z) - \Psi^b$ we have the symmetric case and when $\Psi(-z) - \Psi^b = -(\Psi(z) - \Psi^b)$ the order parameter is antisymmetric. An example of the first is the concentration of, e.g., a homopolymer adsorbing on both surfaces equally. (It turns out that in this case the square root of the polymer concentration is the order parameter.[9])

* Address correspondence to this author.
† Wageningen University.
‡ St. Petersburg State University.
§ Bayer CropScience AG.
⊥ Bayer Technology Services GmbH.

10.1021/jp061299w CCC: $33.50
Published on Web 04/08/2006

Antisymmetric order parameters are found, for example, for surfactant systems where the anisotropic orientation of the molecules in the self-assembled mono- or bilayers is the key variable. (ii) When both surfaces are identical we have to deal with the symmetric boundary conditions, and when the two surfaces have complementary characteristics with respect to the molecules that interact with them, we have the antisymmetric boundary case. Therefore, for colloidal stability problems the symmetric case mostly is relevant for homocoagulation, whereas for heterocoagulation the antisymmetric boundary condition should be used. In accordance with general experience we expect attraction either for a symmetric order parameter in combination with symmetric boundary conditions or for an antisymmetric order parameter using antisymmetric boundaries, and repulsion otherwise.[8]

The Ginzburg−Landau−De Gennes analysis is strictly only applicable for weakly interacting systems. It is tempting, however, to extrapolate the findings to strongly interacting systems. In this paper we will argue that this is not straightforward for surfactant systems.

At surfactant concentrations near the concentration where they self-assemble and form micelles in the bulk solution (the CMC), they typically form self-assembled layers at interfaces through a cooperative adsorption process.[3] When the surfaces are hydrophobic, adsorbed monolayers are formed with the hydrophobic part of the surfactants oriented toward the surface and the hydrophilic part directed toward the aqueous solution, whereas on hydrophilic surfaces a bilayer configuration is found composed of two oppositely oriented surfactant layers. This orientation of the surfactants (normal to the surfaces) is essential. When we bring two identical surfaces together we expect at close proximity that there is some destructive interference with respect to the surfactant orientation. As a result one anticipates repulsive interactions, which are typically referred to as steric forces, but may as well be correlated to the compression of the surfactant layer. Due to this, surfactants are popular additives to improve the colloidal stability.[3]

From the above it is evident that for symmetric boundary conditions one has the option to simplify the computations by taking only the positive coordinates ($z > 0$) into account and impose reflecting boundary conditions at $z = 0$ to include the mirror-image part of the system (at negative z). In numerical analysis this procedure is less expensive CPU-wise and in fact this Ansatz is common practice.[6,10,11] Below we will report on a statistical thermodynamical analysis for surfactants at interfaces wherein the full range $-H/2$, ..., 0, ..., $H/2$ is considered. For large H there is a surfactant monolayer on each surface. However, for strongly confined surfactant layers it appears that there are situations where it becomes favorable for the system to remove one of the surfactant layers such that the remaining layer is less compressed, rather than to compress both layers equally. As a result a confinement-induced symmetry breaking takes place. This has important consequences. A key implication of the uneven distribution of the surfactants over the two surfaces can be understood from the symmetry arguments used above. Instead of symmetric boundary conditions, one now effectively has antisymmetric ones. As a result even the sign of the interaction is affected.

Within the phenomenological Ginzburg−Landau−De Gennes analysis one can only simulate the symmetry breaking by an ad hoc switching of the boundary conditions. Only for molecularly realistic model calculations one can expect to do better. Such theory should reproduce the cooperative adsorption of surfactants at interfaces (near the CMC) as the result of the molecular architecture of the surfactants in combination with the relevant interaction parameters. The self-consistent field approach has these specifications, but in previous considerations one typically simplified the problem by imposing the spatial symmetry in the system.[10,11,13] After we recognized that this is a dangerous practice, we found from our calculations that uneven distributions of surfactants occur in many cases where there is a strong confinement in combination with a cooperative adsorption transition. That is why we now believe that it is a fundamental property of confined surfactant films.

The aim of this paper is to illustrate the symmetry breaking. We do this by choosing a relatively simple model system, i.e., the nonionic surfactant $C_{12}E_6$ in a low molecular weight solvent (water) in combination with apolar surfaces. The SCF theory has been used before for the modeling of surfactants in solution,[14,15] at interfaces,[15−21] and in confined spaces.[10,12,13,16] We will only discuss the basic concepts of the model and its parameters and for more details the above references can be consulted. The free energy of interaction is accurately available from the calculations and therefore we can discuss in the results section all the details relevant for the interaction curves for these surfactant systems in both the symmetry and the symmetry-broken cases. Some dynamical consequences are discussed at the end of the paper. Our predictions may be of help to understand the complex results found for surface force experiments (using an atomic force microscope or the surface force apparatus).[2,22−25]

Self-Consistent Field Theory

At present it is impossible to solve the partition function for molecular models of surfactant self-assembly rigorously. For many systems the next to best strategy is to apply the statistical thermodynamic machinery to computer simulations such as molecular dynamics (MD) or Monte Carlo (MC) implementing molecularly realistic models. Although various observables can be simulated accurately, it is hard to evaluate thermodynamic parameters with high accuracy. As a consequence it is difficult to judge whether particular states of the system correspond to the thermodynamic equilibrium state or are (transient) metastable states. In other words, if long-lived metastable states exist, it is extremely hard to find the average behavior accurately. This problem appears particularly relevant for strongly confined surfactant systems. Here we choose to (numerically) solve an approximate partition function for a molecular realistic model by applying the mean-field approximation leading to a so-called self-consistent field (SCF) analysis. With this theory the mean-field partition function is accurately evaluated and as a result all (mean field) thermodynamic potentials are evaluated up to high precision. With these we can generate the free energy of interaction of both stable as well as metastable states of the system for a given confinement. Even though results can only be generated numerically we note that the CPU times for the SCF calculations are 4 to 5 orders of magnitude lower than corresponding simulations.

As we are going to solve the SCF equations numerically we have to discretise space, i.e., use a lattice. Lattice sites have the linear dimension a. We consider two flat interfaces, which are composed of units of type S. As we will no longer impose the symmetry, even when the surfaces are identical, we might as well choose our coordinate system such that one surface is positioned at $z = 0$ and the other one at $z = H + 1$, and thus the distance between the surfaces is Ha. Layers of lattice sites run parallel to the surface and have ranking numbers $z = 1, 2,$ ..., H. It is convenient to model the solvent and the surfactant

molecules to be composed of segments that exactly fit the lattice sites. Here we take one particular nonionic surfactant $C_{12}E_6$ and choose to follow Barneveld[26] and describe the surfactant on the united atom level: the segment C refers to CH_3 or CH_2 and E refers to ethylene oxide or in the segment notation $(O)_1(C)_2$ where O refers to the oxygen and thus $C_{12}E_6 = (C)_{12}((O)_1(C)_2)_6(O)_1$. The segments in the chain have ranking numbers $s = 1, ..., N$, where in this case $N = 31$. Water is modeled as a molecule with segment type W and each water molecule occupies two neighboring sites. The molecules are distributed onto the lattice. Then for each of the segment types X = C, O, W the average volume fraction $\varphi_X(z)$ is computed at each coordinate, by determining the probability that a lattice site is filled by the segment type. These volume fraction profiles are used in the partition function, which effectively implies that we are going to ignore concentration fluctuations along the surface. Conjugated to the volume fraction profiles there exists corresponding self-consistent potential profiles for each segment type:

$$u_X(z)/k_BT = u'(z) + \sum_Y \chi_{XY}\langle \varphi_Y(z) - \varphi_Y{}^b \rangle \qquad (1)$$

where $u'(z)$ is a Lagrange field contribution coupled to the incompressibility constraint

$$\sum_X \varphi_X(z) = 1 \; \forall \; z \qquad (2)$$

and a similar condition applies in the bulk. The second term in eq 1, in which the sum runs over all segment types including the surface, accounts for the nonideal interactions. It is evaluated by using the Bragg−Williams approximation where the interactions are parametrized by short-range Flory−Huggins nearest-neighbor exchange energy parameters χ.[27] At the end of this paragraph we will go into the values used for these parameters. The angular brackets signal a three-layer average $\langle x(z)\rangle = (x(z-1) + x(z) + x(z+1))/3$. Physically it means that the segments at coordinate z have interactions with segments that sit at $z-1$, z, and $z+1$. The normalization of the interaction term by $\varphi_Y{}^b$ is included to set the segment potentials in the bulk to zero (reference state).

The target of the SCF calculations is to find those volume fraction profiles that optimize the partition function. These profiles follow from the statistical weight of all possible and allowed conformations of the molecules. Conformations are generated with use of a Markov approximation. Within this approximation chains have a finite memory of their path. This rather primitive chain model is attractive for at least two good reasons. First of all, within this approach the intrachain excluded-volume effects are treated on the same footing as the interchain excluded-volume ones. Second, there exists a very efficient propagator scheme to generate the full set of statistical weights for all possible conformations of the molecules. The start of this efficient scheme is to define segment-type dependent Boltzmann factors $G_X(z) = \exp(-u_X/k_BT)$, which are generalized to ranking number dependent quantities $G_i(z,s) = \sum_X G_X(z)\delta_{i,s}{}^X$, where $\delta_{i,s}{}^X = 1$ when segment s of molecule i is of type X and zero otherwise. Using these Boltzmann factors it is possible to generate two complementary end-point distribution functions $G_i(z,s|1)$ and $G_i(z,s|N)$ by the recurrence relations

$$G_i(z,s|1) = G_i(z,s)\langle G_i(z,s-1|1)\rangle \qquad (3)$$

$$G_i(z,s|N) = G_i(z,s)\langle G_i(z,s+1|N)\rangle \qquad (4)$$

which are started by $G_i(z,1|1) = G_i(z,1)$ and $G_i(z,N|N) = G_i(z,N)$, respectively. The angular brackets again refer to a three-layer average. Physically $G_i(z,s|1)$ collects the statistical weight of all possible conformations from the free chain end $s = 1$ to segment s at coordinate z and a similar meaning can be assigned to $G_i(z,s|N)$. The volume fraction profile is generated by the composition law:

$$\varphi_i(z,s) = C_i \frac{G_i(z,s|1)G_i(z,s|N)}{G_i(z,s)} \qquad (5)$$

where C_i is a normalization constant. This constant is linked to the bulk volume fraction $C_i = \varphi_i{}^b/N_i$ and determines the number of segments (per unit area) in the system:

$$\theta_i = \sum_s \sum_z \varphi_i(z,s) = C_i N_i \sum_z G_i(z,1|N) \qquad (6)$$

The excess adsorbed amount is easily evaluated by $\theta_i{}^\sigma = \theta_i - H\varphi_i{}^b$, and the volume fractions for a given segment type follow from $\varphi_X(z) = \sum_i \sum_s \varphi_i(z,s)\delta_{i,s}{}^X$.

It can be shown that the partition function is optimized as soon as the potentials are consistent with the volume fraction profiles (provided the system obeys the incompressibility constraint). For the SCF solution it is true that the volume fractions that determine the potentials are recovered by the propagator procedure.

High precision (up to at least 7 significant digits) SCF solutions are routinely generated by a numerical algorithm (using only seconds of CPU on a 2 GHz PC). For such SCF result not only are the volume fraction distributions available, but it is also possible to compute all thermodynamic properties accurately. Below we will be interested in the free energy of interaction for the case that the chemical potential of the molecular components is fixed. The relevant thermodynamic potential in this case is the grand potential $\Omega \equiv F - \sum_i n_i\mu_i = k_BT\sum_z \omega(z)$. Here F is the Helmholtz energy, $n_i = \theta_i/N_i$ is the number of molecules, and μ the chemical potential. The dimensionless grand potential density $\omega(z)$ can be computed by:[28]

$$\omega(z) = -\sum_i \frac{\varphi_i(z) - \varphi_i{}^b}{N_i} - u'(z) - \frac{1}{2}{\sum_{X,Y}}' \chi_{XY}(\varphi_X(z)\langle\varphi_Y(z)\rangle - \varphi_X{}^b\varphi_Y{}^b) \qquad (7)$$

where the prime on the sum sign indicates that in the sum the surface component is not included. In this equation we have chosen to distribute the nonlocal contribution to the grand potential evenly over the segments involved. This choice has no consequence for the overall grand potential.

The free energy of interaction per unit area is now found by:

$$F^{int}(H) = \Omega(H) - \Omega(\infty) \qquad (8)$$

This free energy of interaction is expected to be the leading contribution to the overall free energy of interaction. It is understood that one should add additional contributions to the free energy of interaction, such as the van der Waals attraction, on top of this (using the usual superposition approximation).

We conclude by paying attention to the appropriate choices for the short-range interaction parameters. In an incompressible system it is possible to choose the reference of the interaction energy such that only contacts between unlike segments have to be counted. There are three parameters important for the self-

assembly of the surfactants in the bulk, i.e., the repulsion between the hydrophobic units and water drives the self-assembly. We choose the value $\chi_{CW} = 1.5$. The effective solvency parameter for the interaction of the E headgroup with water should be sufficiently good so that the heads are well solvated and contribute to the stopping force for self-assembly. As in each E there are two C's and we need a negative value for the O−W contacts. We choose $\chi_{OW} = -0.6$. Finally, it is important that there is some repulsion between heads and tails. Consistent with previous studies we take $\chi_{CO} = 2.2$. This set reproduces almost quantitatively the trends in CMC for a large set of C_nE_m surfactants (around room temperature) that feature an exponential drop in the CMC with increasing n, and a very small increase in CMC with increasing m.[29] We will not go into these details and mention that the CMC for $C_{12}E_6$ is φ^b-(CMC) = 0.0002, which corresponds to a concentration of about $c \approx 0.0003$ mol/L. For this conversion we needed a value for the length of a lattice site. Consistent with the use of united atoms we take $a = 0.3$ nm. We note that the results reported below only qualitatively change when these parameters are varied (within limits of course). In principle there are also three interaction parameters that specify the interactions of the molecular species with the surface S. However, because the volume fraction distribution of S is fixed (to $\varphi_S(z) = 1$ for $z < 0$ and $z > H$ and 0 otherwise), it can be shown that it is possible to set one parameter to zero (we choose $\chi_{SW} = 0$) and only specify the remaining two. The most simple case for surfactant adsorption is found for hydrophobic surfaces. Parameters consistent with this are $\chi_{SC} = -0.9$ and $\chi_{SO} = 3$: the tails are effectively attracted and the heads are repelled from the surface. We will see below that this set gives significant adsorption of the surfactant at the CMC. We note that for a direct comparison to experiments it is necessary to tune the adsorption parameters. We will not do this here and mention again that there is a wide range of parameters for which qualitatively the same occurs as is discussed below.

Below we will discuss adsorption isotherms of surfactants as a function of the confinement. In such an isotherm one plots the excess amount of surfactant at the surface as a function of the logarithm of the surfactant concentration in the bulk (chemical potential). Starting from the CMC, the surfactants form micellar objects in solution. Increasing the bulk concentration of free surfactants above the CMC value is accompanied by an exponential growth of the concentration of micelles. Moreover there may exist chemical potentials higher than the chemical potential at which the CMC occurs at which the system rather abruptly decides to form linear micelles or vesicles (second CMC). In any case, the possibilities to increase the free surfactant concentration above the value of the second CMC are even more difficult. In the SCF calculations it is possible to consider the adsorbed layer for chemical potentials above the CMC because in such calculations the micelle formation in the bulk is suppressed. One should keep in mind, however, that for practical systems the concentration of free surfactants above the CMC value is limited and that the isotherms effectively terminate at bulk volume fractions that are slightly above the CMC.

Results

Two Surfaces Far Apart. Let us start by discussing a pair of adsorption isotherms $\theta^\sigma(\log\varphi^b)$ of the nonionic surfactant $C_{12}E_6$ onto two hydrophobic surfaces at a separation far enough such that the two surfactant layers do not interact with each other. In Figure 1a the result is given for the case that symmetry

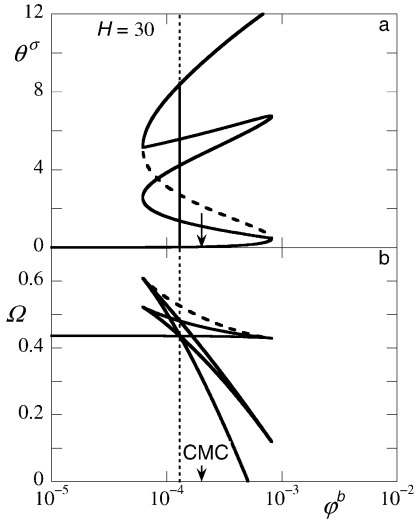

Figure 1. (a) The excess amount of surfactant (in equivalent monolayers on both surfaces) as a function of the logarithm of the bulk volume fraction of surfactants. (b) The grand potential (in units of k_BT/a^2) as a function of the logarithm of the bulk volume fraction of surfactants. The solid line refers to the case where the surfactants are allowed to distribute unevenly. The dashed line is where a symmetric distribution is enforced. The distance between the surfaces is $H = 30$ (in lattice units a). The vertical dotted line is positioned at the binodal of the surface phase transition. The arrows point to the CMC.

is enforced in the system (dashed line) together with the result that is found when the system can choose to, but not necessarily does, distribute the surfactants unevenly over the surfaces (solid line). Both at very low as well as very high adsorbed amounts there is no difference between the two calculations (the solid line hides the dashed one). In the intermediate adsorbed amounts there is a significant difference. In Figure 1b the corresponding grand potential is plotted versus the logarithm of the bulk volume fraction of the surfactant. Referring to the symmetric case, the isotherm has a large van der Waals loop and the corresponding grand potential curve has a cusped structure. The binodal of the transition is found for the condition that the two coexisting interfacial layers have the same grand potential and the same chemical potential for the surfactant. This point is easily recognized in Figure 1b where there is the crossing of the lines. The dotted vertical line is positioned at the transition point (binodal). Consequently, the adsorption isotherm features a jump-like increase in the adsorbed amount at the binodal. At this jump the almost empty surfaces are abruptly covered by a monolayer. In the monolayer the surfactant has the hydrophobic parts directed toward the surface and the hydrophilic part points toward the solution.

For the antisymmetric case (unevenly distributed surfactants) the isotherm shows a complex double van der Waals loop and the corresponding grand potential curve has two times two cusps, indicating two transitions. The binodals of the two transitions coincide with each other and with the binodal of the symmetric case. Therefore, the isotherm shows exactly the same jumps for both situations and the equilibrium state is the same and identical with the symmetric situation. If the chemical potential at which the adsorption transition occurs is seen as some energy level, we would interpret this result as a double degenerate energy level. Below we will see that this degenerate state no longer occurs when the surfactant layers interact with each other.

Associated with each binodal there are two spinodal points. These points are recognized in Figure 1b by the two cusps and these correspond in Figure 1a to the points where $\partial\log\varphi^b/\partial\theta^\sigma = 0$. From the binodal to the first spinodal point and from the

second spinodal point to the binodal the system is metastable. The two adsorption isotherms match just as in the stable situation. Although the system is not forced to remain symmetric, the symmetric distribution of the surfactant over the two surfaces is the only solution of the SCF equations. Here we stress again that the binodals of both loops of the symmetry-broken adsorption isotherm occur at exactly the same chemical potential as that of the symmetry-enforced isotherm. As the surfaces are far apart ($H = 30$) the two adsorbed layers do not feel each other, both monolayers become thermodynamically stable at exactly the same chemical potential and the spinodal points also match. This implies that both monolayers also lose the metastability at exactly the same chemical potentials and also that the metastability of the (almost) bare surface is lost at the same chemical potential.

For the region where the symmetric system is unstable, the part where the dashed line is visible, the two isotherms differ. In other words, the system makes use of the extra degree of freedom to distribute the surfactants unevenly over the two surfaces. Exactly at the spinodal points the curve, corresponding to the broken symmetry, kinks away from the symmetric one. This implies that the symmetry breaking per se is a second-order phase transition. The first of the two consecutive van der Waals loops corresponds to the formation of the monolayer on only one of the surfaces, and the second one corresponds to the formation of the second monolayer on the other surface. The reason the two loops are very different is that the second monolayer is formed in the presence of the first one: in the unstable part of the second loop some molecules swap from the first monolayer to the second one. This is the reason the second van der Waals loop is not classical: even in the unstable part of the curve $\partial\theta^{\sigma}/\partial\log\varphi^{b} > 0$. The reason for the symmetry breaking is also evident. At the first spinodal point the system can choose either to construct two equally unstable monolayers or to get as "quickly" as possible away from instability by using all the surfactants to form the first stable monolayer. As the total amount of instability is reduced, the system chooses for this. In Figure 1b the preference of making one monolayer after the other, over making two monolayers simultaneously, is seen from the fact that the grand potential of the unstable part in the symmetric case is higher than that of the symmetry-broken system.

Two Surfaces in Close Proximity. The next step is to show how the adsorption isotherms and the grand potential curves change upon decreasing the spacing between the surfaces. In Figure 2 we show typical results for the distance $H = 10$. Qualitatively there are many similarities with the results of Figure 1, but there are also important quantitative differences. Basically the lower parts of the adsorption isotherms are not much affected by the confinement, and the most pronounced effects are seen in the top parts. This is obvious because the more surfactants there are between the surfaces, the stronger is the overlap of the opposing surfactant layers. As the top part of the isotherms are affected it is not surprising that the positions of the binodals have changed (with respect to the unconfined case). Only the binodal for the formation of the first monolayer (in the asymmetric case) is found at the original position. The binodal for the second monolayer is shifted to much higher chemical potential and also the binodal for the symmetry-enforced isotherm is moved to a higher chemical potential. The spontaneous symmetry breaking at low adsorbed amounts remains in the spinodal point of the isotherms; however, the recovering of the symmetric state at high adsorbed amounts now also moved to higher chemical potentials and no longer occurs

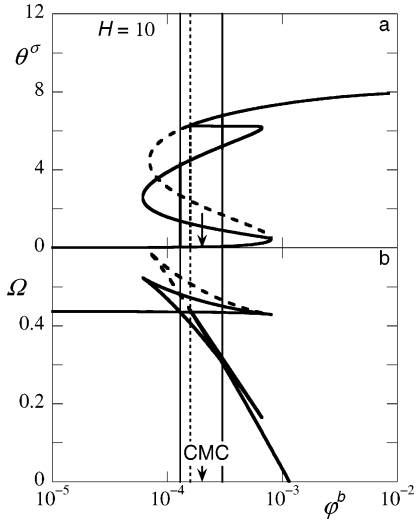

Figure 2. (a) The excess amount of surfactant (in equivalent monolayers on both surfaces) as a function of the logarithm of the bulk volume fraction of surfactants. (b) The grand potential in units of k_BT/a^2, as a function of the logarithm of the bulk volume fraction of surfactants. The solid lines refer to the case where the surfactants are allowed to distribute unevenly. The dashed line applies to the symmetric distribution. The distance between the surfaces is $H = 10$ (in units a). The vertical lines are positioned at the binodals. The arrows point to the CMC.

at the spinodal point of the symmetric adsorption isotherm. Again if the chemical potential at which the surface phase transition occurs is interpreted as some sort of energy level, we see that the close proximity of the two surfaces effectively imposes some external field to the system such that the energy levels split. Recall that the energy level was degenerate in the absence of the confinement field (cf. Figure 1).

It is important to stress that in the strongly confined case the adsorption isotherm has two steps. The first one is connected to the formation of one monolayer (on one of the surfaces), and the second one corresponds to the recovery of the symmetric distribution of segments. The first step occurs well below the CMC; however, the second one is found above the CMC. In practice, one should therefore expect an asymmetric distribution of the surfactants over the two surfaces at the CMC. Indeed, the comparison to the symmetric isotherm reveals that the symmetrically distributed case has a higher grand potential (at the CMC) than the monolayer coverage (cf. Figure 2b).

At this stage it is of interest to show that there is a difference in the molecular distributions that result from imposing the symmetry constraint (cf. Figure 3a) or for the case that the system has the extra degree of freedom of distributing the surfactants unevenly over the surfaces (cf. Figure 3b). Inspection of the profiles given in Figure 3 is instructive. Let us first mention a few general characteristics that are also true for adsorbed monolayers when the surfaces are far apart (symmetrical case). As the surfaces are hydrophobic, we find that the tail segments are enriched near the surfaces. The volume fraction of tail segments is high but remains significantly below unity (see Figure 3a). There are two reasons for this. One reason is that there is some solvent (not shown) even in the hydrophobic regions. Most likely this is somewhat overestimated by the model because the solvent lacks the true self-associating properties of water. The second reason is that there is a significant number of headgroup units close to the surface. Ethylene oxide is a somewhat amphoteric group and the strict separation between heads and tails should not be expected for nonionic surfactants. Most of the headgroup segments, however,

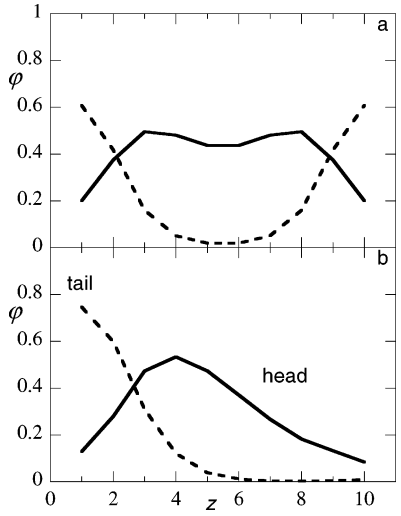

Figure 3. The volume fraction profile of heads (solid lines) and tails (dashed lines) across the gap between two surfaces at a distance $H = 10$ (in units a) with the bulk volume fraction at the CMC: (a) for the case that the distribution is forced to be symmetric and (b) for the case that the distribution is not the same on each surface.

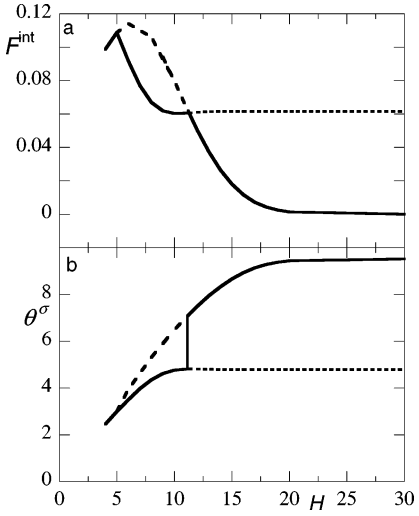

Figure 4. (a) Free energy of interaction (in units of k_BT/a^2) as a function of the distance between the surfaces H (in units a). (b) The corresponding adsorbed amount of surfactants (in equivalent monolayers for both surfaces) as a function of the distance between the two surfaces. The solid lines represent the equilibrium curve. The dashed curve is what is found when the symmetry is enforced in the system. The dotted curve is the metastable part of the symmetry-broken system for large distances.

are predominantly found away from the surface on the aqueous side of the adsorbed monolayer.

From Figure 2 we know that in the confined situation the uneven distribution (cf. Figure 3b) has a lower grand potential at the CMC than the symmetric one (cf. Figure 3a). From inspection of the profiles one can find clues that are consistent with this thermodynamic finding. In the symmetric profile there is a very strong overlap of headgroups in the center of the system. The headgroups are pushed somewhat into the hydrophobic domains. The two compressed monolayers are therefore effectively thinner than the less compressed monolayer in the symmetry-broken system. By changing to the less compressed state the system is relaxed. In passing we note that the uneven distribution of surfactants as shown in Figure 3b can be compared with the situation at the binodal (at a large separation), where also a sparsely covered surface is in equilibrium with an adsorbed monolayer.

Free Energy of Interaction and Regulation of the Adsorbed Amount. The free energy of interaction and the adsorbed amount in the gap are computed, while fixing the chemical potential (bulk volume fraction) of the surfactant to the CMC value. From an experimental point of view this chemical potential is the easiest one to control. This means that upon changes in the distance between the particles H the amount of surfactant adsorbed and their distribution over both surfaces may change and this will affect the free energy of interaction. As told above the grand potential is the characteristic function in this case and the free energy of interaction $F^{int}(H)$ is computed with use of this quantity. The system with two monolayers (one at each surface) at large separation is used as the reference for the free energy.

In Figure 4a two interaction curves are presented: one computed with the constraint of symmetry (dashed line), the other one without this constraint (dotted line). We use the solid line for those results that represent the lowest free energies. At large separation the symmetric system has the lowest free energy (dashed → solid). The dotted curve at large separation thus corresponds to the metastable symmetry-broken system. The two curves intersect at the transition distance $H \approx 11.3$ and the uneven distribution becomes the most favorable one (dotted → solid) up to $H \approx 5$. At $H \approx 6$ the free energy of interaction for the symmetric case goes through a maximum just before it meets the symmetry-broken system. Beyond this point ($H < 5$) the symmetrical situation prevails, the adsorbed amount decreases and the interaction force declines (data for $H < 4$ are omitted). It is important to note that at both distances ($H = 5$ and 11.3), where the equilibrium adsorbed layers switch their structure symmetry-wise, the force $f = -\partial F^{int}/\partial H$ has different signs. This is most easily seen for the merging of the lines at $H = 5$. The symmetric system has an increasing trend with increasing distance, i.e., the force is negative, whereas the symmetry-broken system departs from this line with a negative slope, which corresponds to a positive force. Also at $H \approx 11.3$ this phenomenon occurs. Close inspection shows that the force is weakly negative (attraction) for the symmetry-broken line, whereas the force is positive (repulsion) for the symmetric system. This difference is important. It shows that the system uses the extra degree of freedom to instantaneously change the sign of the interaction.

In Figure 4b the corresponding results are shown for the amount of surfactant that sits within the gap as a function of the distance between the surfaces. Again, this figure is composed of two curves, one computed from the symmetry-enforced case and the other one where the distributions of the surfactants can vary between the surfaces. We represent the system with the lowest free energy with a solid line (equilibrium situation) and the metastable line parts are dashed (symmetric profile) or dotted (asymmetric profile). In both curves we basically see that the adsorbed amount is an increasing function of the distance H. At large values of separation, the adsorbed amount saturates to a plateau, but the system with one monolayer has half the adsorbed amount of that where there are two monolayers (one at each surface). At large distance there is room enough for a monolayer structure on both surfaces and this is the stable (equilibrium) situation. A sudden transition occurs at distance $H \approx 11.3$. The adsorbed amount drops by a significant amount as in equilibrium one of the monolayers is removed such that the remaining one has more space. This situation prevails until $H = 5$. At very short separation there is very little room for adsorption and both surfaces become symmetrically populated.

We showed that at both $H = 5$ and 11.3 the equilibrium force has a kink and as a result these distances point to two confinement-induced phase transitions. The transition at $H = 11.3$ is first order because it is accompanied by a jump in the adsorbed amount, whereas the transition at $H = 5$ is second order because the adsorbed amount does not jump.

Discussion

Adsorption isotherms as reported in Figures 1 and 2 can in principle be measured, but a systematic analysis of such isotherms as a function of the confinement parameter H will be a formidable task (although adsorption of surfactants in porous media can be determined[30]). The same applies for the volume fraction profiles as shown in Figure 3. In principle one can determine those by using a neutron scattering technique. However, the systematic analysis where the confinement H is set to the dimensions comparable to the thickness of the surfactant layers is very tricky.[31] However, monitoring surface forces is becoming routine using the surface force apparatus or various versions of the atomic force microscope.[1,2] In an experiment that is conducted infinitely slow such that the equilibrium curve is recorded, we expect that upon the decrease of the distance between the surfaces there is a confinement-induced phase transition, which is accompanied by a large change in the amount of surfactants within the gap as explained above. In experiments, however, it is difficult to probe thermodynamic equilibrium forces, and we have to consider the possibility that the system probes metastable parts in the free energy landscape. An interesting dynamic hysteresis scenario presents itself.

Let us assume that a surface force experiment is conducted at such a speed that the system has no time to make large (spontaneous) changes in the adsorbed amount, but that it exchanges surfactants according to some local equilibration process. Then we can imagine that the system will start with two monolayers, one at each surface. Upon compression the system loses surfactants gradually, but remains symmetric all the way to very small distances. In other words, the system does not notice the need to switch to the symmetry-broken state. However, when from the highly confined state the system is at $H = 5$ and the increase in distance takes place, the system can easily go into the asymmetric branch, because after all it represents is the lowest free energy in the system and there are no jumps in uptake of surfactants needed to go into this branch (second-order phase transition). When the distance is increased there is a gradual uptake of surfactants and even above $H = 11.3$ the system does not notice that it is more favorable to have two monolayers (one on each surface) in the system and the symmetry-broken state persists up to large separations. As a result there is a strong hysteresis in this system that can be realized without the need to have a large jump in the adsorbed amount. Most likely under experimental situations one will follow this scenario to some extent, but at some point the system must return to the static result. As a result, we anticipate quite complex results of surface force experiments on surfactant systems. These notions are confirmed by various available results of force measurements of surfactant layers with surface force equipment.[2,22−25]

In the above we have assumed that the two surfaces are identical. Real macroscopic surfaces are likely to be at best quasi-indentical due to possible lateral inhomogeneities in surface properties. However, surfactant layers, especially in the case that the surfactants form closed mono- or bilayers, mask these lateral inhomogeneities and the symmetry-breaking scenario should therefore be expected also for systems with less ideal substrates.

We will conclude this paper with a few remarks regarding the use of the SCF theory for surfactant systems. The key approximation in the SCF theory is that the actual binary interactions are replaced by interactions of a segment with a self-consistent potential. It is known that for densely packed molecular arrangements this mean-field approximation is very good. The reason is that each molecule interacts with many of its neighbors and therefore the average surrounding (which is mimicked by the potentials) does not deviate much from the actual one. This is the reason, e.g. the SCF results follow all-atom molecular dynamics simulations for the case of the lipid bilayer membrane, in very large detail.[32,33] For surfactant adsorption, however, there are several additional factors one has to keep in mind. By far the most relevant problem is that the theory does not allow for some lateral structure in the surfactant layers. Indeed, for most adsorbed surfactant layers experiments tell us that the homogeneous film is rare and should only be expected for those surfactants that form lamellae with high preference.[34,35] In this paper we choose the nonionic $C_{12}E_6$, which most likely does not form fully compact monolayers at hydrophobic surfaces. However, even when the surfactant layers are broken to some extent, we still expect that our predictions hold qualitatively. The obvious modification is that the symmetry breaking takes place locally and the overall symmetry is restored at larger length scales. More specifically, we expect that, at some confinement, parts of the monolayer of one surface and parts of the monolayer on the other surface will disappear in a correlated way, meaning that at each specified lateral position (x, y) there exists a surfactant aggregate only on one of the surfaces. Obviously, such broken structure of the monolayer has kinetic consequences, because it is expected that such a system can respond significantly quicker to the changes in confinement than the systems that have intact monolayers. To construct a full (dynamic) theory that accounts for these lateral fluctuations, needed for a full understanding of the experimental systems, is definitely a challenge for years to come.

Conclusions

Adsorbed surfactant layers have a thickness comparable to the length of the surfactants. When two surfaces, coated with surfactant layers, are brought to a distance comparable to the surfactant length the system can choose between having two compressed surfactant layers or having just one layer (attached to one of the surfaces) that is more relaxed. In other words the optimization of the surfactant layer on one surface may lead to the loss of the layer at the other surface. We have shown, by SCF calculations for a molecular model, that a region of confinement exists for which the latter scenario is favorable from a free energy perspective. The breaking of the symmetry and the restoration of it have the effect that the surface forces change sign. This means that repulsion switches to attraction (in the compression mode) and visa versa (in the expansion mode) when such transition takes place. This has important consequences for systems in which surfactants have the duty to mediate the intermolecular and surface forces. We have discussed the scenario that in dynamic experiments there is a hysteresis between forces measured upon compression and expansion. Remarkably, such hysteresis can be found without the need to have a jump-like change in the amount of surfactants in the confined region. We have illustrated this behavior for a simple system of a nonionic surfactant in water, but mention that it is not limited to this. A prerequisite for confinement-

induced symmetry breaking is that the systems must have some sort of cooperative adsorption process. Ionic surfactants at (charged) hydrophilic surfaces and copolymers in selective solvents are other examples.

References and Notes

(1) Israelachvili, J. N. *Intermolecular and surface forces*; Academic Press: New York, 1992.
(2) Butt, H.-J.; Capella, B.; Kappl, M. *Surf. Sci. Rep.* **2005**, *59*, 1.
(3) Evens, D. F.; Wennerstrom, H. *The colloidal domain where physics, chemistry, biology and technology meet*; VCH Publishers: New York, 1994.
(4) Deryagin, B. V.; Landau, L. D. *Acta Physicochem. U.R.S.S.* **1943**, *14*, 633.
(5) Verwey, E. J. W.; Overbeek, J. Th. G. *Theory of the Stability of Lyophobic Colloids*; Elsevier: New York, 1948.
(6) Fleer, G. J.; Cohen Stuart, M. A.; Scheutjens, J. M. H. M.; Cosgrove, T.; Vincent, B. *Polymers at Interfaces*; Chapman and Hall: London, UK, 1993.
(7) Helfrich, W. *Elasticity and thermal undulations of fluid films of amphiphiles*: *Liquids at interfaces*; Charvalin, J., Joanny, J. F., Zinn-Justin, J., Eds.; Les Houches: Berlin, Germany, 1988.
(8) Landau, L. D.; Lifshitz, E. M.; Pitaevskii, L. P. *Statistical Physics. Part 1*; Pergamon Press: Oxford, UK, 1980.
(9) De Gennes, P.-G. *Scaling Concepts in Polymer Physics*; Cornell University Press: Ithaca, NY, 1979.
(10) Lokar, W. J.; Koopal, L. K.; Leermakers, F. A. M.; Ducker, W. A. *J. Phys. Chem. B* **2004**, *108*, 15033.
(11) Scheutjens, J. M. H. M.; Fleer, G. J. *Macromolecules* **1985**, *18*, 1882.
(12) Lokar, W. J.; Koopal, L. K.; Leermakers, F. A. M.; Ducker, W. A. *J. Phys. Chem. B* **2004**, *108*, 3633.
(13) Leermakers, F. A. M.; Koopal, L. K.; Lokar, W. J.; Ducker, W. A. *Langmuir* **2005**, *21*, 11534.
(14) Leermakers, F. A. M.; Scheutjens, J. M. H. M. *J. Chem. Phys.* **1988**, *89*, 3264.
(15) Böhmer, M. R.; Koopal, L. K.; Lyklema, J. *J. Phys. Chem.* **1991**, *95*, 9569.
(16) Koopal, L. K.; Leermakers, F. A. M.; Lokar, W. J.; Ducker, W. A. *Langmuir* **2005**, *21*, 10089.
(17) Böhmer, M. R.; Koopal, L. K.; Janssen, R.; Lee, E. M.; Thomas, R. K.; Rennie, A. R. *Langmuir* **1992**, *8*, 2228.
(18) Goloub, T. P.; Koopal, L. K. *Langmuir* **1997**, *13*, 673.
(19) Böhmer, M. R.; Koopal, L. K. *Langmuir* **1990**, *6*, 1478.
(20) Böhmer, M. R.; Koopal, L. K. *Langmuir* **1992** *8*, 1594.
(21) Lee, E. M.; Koopal, L. K. *J. Colloid Interface Sci.* **1996** *177*, 478.
(22) Clark, S. C.; Ducker, W. A. *J. Phys. Chem. B* **2003** *107*, 9011.
(23) Grant, L. M.; Tilberg, F.; Ducker, W. A. *J. Phys. Chem. B* **1998**, *102*, 4288.
(24) Grant, L. M.; Ederth, T.; Tilberg, F. *Langmuir* **2000**, *16*, 2285.
(25) Grant, L. M.; Ducker, W. A. *J. Phys. Chem. B* **1997**, *101*, 5337.
(26) Barneveld, P. A.; Scheutjens, J. M. H. M.; Lyklema, J. *Langmuir* **1992**, *8*, 3122.
(27) Flory, P. *Principles of Polymer Chemistry*; Cornell University Press: Ithaca, NY, 1953.
(28) Evers, O. A.; Scheutjens, J. M. H. M.; Fleer, G. J. *Macromolecules* **1990** *23*, 5221.
(29) Tanford, C. *The hydrophobic effect*: *formation of micelles and biological membranes*; J. Wiley and Sons, Inc.: New York, 1973.
(30) Woywod, D.; Schemmel, S.; Rother, G.; Findenegg, G. H.; Schoen, M. *J. Chem. Phys.* **2005**, *122*, 124510.
(31) Cosgrove, T.; Zarbakhsh, A.; Luckham, P. F.; Hair, M. L.; Webster, J. R. P. W. *Faraday Discuss.* **1994**, *98*, 189.
(32) Rabinovich, A. L.; Ripatti, P. O.; Balabaev, N. K.; Leermakers, F. A. M. *Phys. Rev. E*: *Stat., Nonlinear, Soft Matter Phys.* **2003**, *67*, 011909.
(33) Leermakers, F. A. M.; Rabinovich, A. L.; Balabaev, N. K. *Phys. Rev. E*: *Stat., Nonlinear, Soft Matter Phys.* **2003**, *67*, 011910.
(34) Ducker, W. A. Atomic Force Microscopy of Adsorbed Surfactant Micelles. In *Adsorption and Aggregation of Surfactants in Solution*; Mittal, K. L., Shah, D. O., Eds.; Marcel Dekker: New York, 2003.
(35) Jódar-Reyes, A. B.; Ortega-Vinuesa, J. L.; Martin-Rodriguez, A.; Leermakers, F. A. M. *Langmuir* **2003**, *19*, 878.